Journal of Engineering Science and Technology
6th EURECA 2016 Special Issue May (2017) 71 - 83

EFFECT OF ATMOSPHERIC ALTITUDE ON THE DRAG OF WING AT SUBSONIC AND SUPERSONIC SPEEDS

ABDULKAREEM SH. MAHDI AL-OBAIDI, JUSTIN XIAN YUEN MOO*

School of Engineering, Taylor's University, Taylor's Lakeside Campus,
No. 1 Jalan Taylor's, 47500, Subang Jaya, Selangor DE, Malaysia
*Corresponding Author: jusm12@hotmail.my

Abstract

Drag produced by a wing is always aimed to be reduced or kept low. Unfavourable drag force means additional effort is required to carry out work, which reduces the efficiency of the wing. Three of the variables affecting the drag force experienced by a wing are the condition of fluid that it is operating in, the travelling velocity and the drag coefficient which depends on the wing's aerodynamic geometry. The operational condition of missile involves rapid gain in altitude; hence the effect of altitude is the most significant for missile flight compared to other aerial vehicle. Operational speed of missile ranges from subsonic to supersonic where the occurrence of shock wave causes an increase in drag coefficient; hence the drag coefficient is inaccurate to be considered as a constant. Study was carried out to determine the effects of altitude on the three variables which determine the drag force. Through analytical approach, the factors affecting were caused by the changing air parameters with altitude. Atmospheric modelling is developed according to the International Standard Atmosphere which considers the earth's atmospheric layer up to 105 km above sea-level. Through calculation, it is determined that the kinematic viscosity of air affects the drag coefficient the most through Reynolds number. The contribution of the atmospheric air density is significant when drag is considered as a force. The effect of attitude on drag coefficient of a wing was increased by 10.8%, 45.8% and 139.2% at 25 km, 50 km and 75 km above sea-level. The results when drag coefficient of the wing is considered as a function to altitude and Mach number were calculated based on semi-empirical formulation. The resultant drag coefficients were used to analyse for trajectory and flight performances using a developed MATLAB computer program. Trajectories with case of zero drag, constant drag and drag varying with altitude and Mach number show significance difference.

Keywords: Drag coefficient, Atmosphere, Altitude, Trajectory, Subsonic, Supersonic, Wing.

Nomenclatures

A	Area, m^2
AR	Aspect ratio
b	Wing span, m
C_{D0}	Zero-lift drag coefficient
C_{Db}	Base drag coefficient
C_{Df}	Skin friction drag coefficient
$C_{D\ Parasite}$	Parasite drag coefficient
C_{Dw}	Wave drag coefficient
C_f	Skin friction coefficient
C_p	Base pressure coefficient
C_w	Theoretical wave drag parameter
c_r	Root chord, m
c_t	Tip chord, m
g	Gravitational force, m/s^2
h	Height, m
Ma	Mach number
m	Mass, kg
P	Pressure, Pa
Re	Reynold's number
S_{Ref}	Referenced area, m^2
$R_{Specific}$	Specific gas constant, $J\ K^{-1}\ kg^{-1}$
S_{wet}	Wing wetted area, m^2
t	Wing thickness, m
T	Absolute temperature, K
v	Volume, m^3

Greek Symbols

Λ_{LE}	Leading edge sweep angle, deg.
μ	Dynamic viscosity, Ns/m^2
ν	Kinematic viscosity, m^2/s
ρ	Density, kg/m^3
ϕ	Wing sweep correction factor

1. Introduction

Air properties such as temperature, pressure, density and viscosity change with altitude. This being that air exists as a form of gas where expansion and compression depends on the atmospheric pressure and temperature. It is known that drag force experienced by a wing depends on the atmospheric condition density and viscosity, hence it is said that the aerodynamic drag experienced by a wing also varies with altitude [1].

Drag force experienced by a wing also depends on the Mach number which is a measurement of speed of the wing travelling relative of the speed of light. It is known that the speed of light changes with surrounding temperature [2], hence it can be said that Mach number varies with altitude. Due to shock wave which contributes significantly towards the drag coefficient when the wing travels near supersonic speed, it is important to consider the overall effects of altitude towards the drag force experienced by a wing [3]. Analysis was carried out by modelling a

trajectory of a missile wing with identical pre-launch setup. By analysing the different flight parameters of the wing throughout flight time, discussion on the effect of altitude towards overall drag experienced by the wing can be carried out.

Studies show that the effect of Reynold's number on the trajectory of a shuttlecock was similarly determined using trajectory as a form of visualization and comparison Personnic et al. [4]. The comparison of trajectory between two types of shuttlecock made of different material which causes the difference in aerodynamics performances through the variation of Reynold's numbers. The study concludes that the variation was caused by the lower drag force experienced by the more flexible shuttlecock, as the flexibility at higher speed reduces the C_{D0} at the base of the shuttle cock, hence causing the overall C_{D0} of the shuttlecock to be lower. This shows the effects of variable C_{D0} at affecting the overall drag force hence the trajectory of a body.

This study uses a baseline configured surface-to-surface missile (SSM) which is a single-wedged wing (Fig. 1) which allows it to operate in both subsonic and supersonic speed [5]. The availability of semi-empirical aerodynamic data of the typical SSM wing allows a more accurate and realistic analysis to be carried out through this study. However, the SSM wing used generally serves as a medium to visualize the effects of altitude towards drag force, further studies can be carried out using different wing or even the consideration of a missile body.

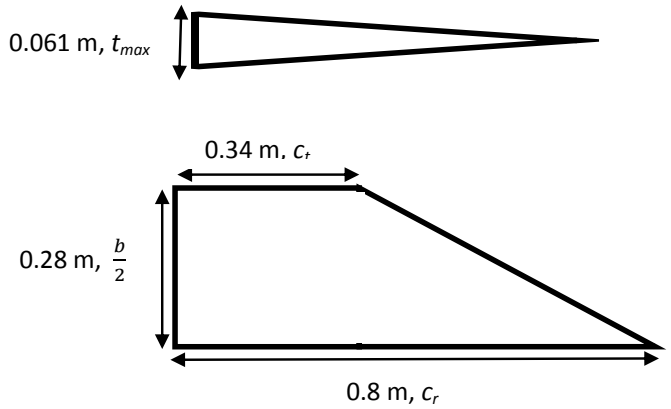

Fig. 1. SSM Configured wing geometry.

2. Prediction of Drag Coefficients

Analytical methods and semi-empirical formulation were used to determine the drag coefficients under different conditions. Data were acquired through Data Compendium (DATCOM) software which combines actual flight data and mathematical formulation in order to provide realistic and reliable estimation of the flight parameter required. Characteristics are adapted from Refs. [6 - 9] and converted to numerical data plotted in graph, as outlined in *Appendix A*.

2.1. Zero-lift drag coefficient C_{D0}

The total zero-lift drag coefficient of the body is usually considered to be of three components, friction drag, wave drag, and base drag as shown in Eq. (1), with wave drag exist at near Mach number 1. These different components are further discussed in the following sub-sections.

$$C_{D0} = C_{Dfr} + C_{Dw} + C_{Db} \quad (1)$$

2.1.1. Friction drag coefficient

The skin friction drag coefficient can be calculated though the following equation with C_{Dfr} known as the skin friction coefficient of the wing. C_f is the primary skin friction factor determined through the Prandtl-Schlichting [10]. The equation considers the wing thickness factor, η_t. The area of the wing wetted, S_{Wet} by the air which can be directly related to the skin friction factor [11], this shows that the wing geometry is considered in determining friction drag coefficient.

$$C_{Dfr} = C_f \eta_t \frac{S_{Wet}}{S_{ref}} \quad (2)$$

2.1.2. Wave drag coefficient

Wave drag coefficient exists at speed above subsonic at near Ma = 1 due to shock wave. At this point C_{D0} of the wing increases significantly, typically increasing by a factor of 10 in some cases [12]. The spike in C_{D0} outside subsonic speed is crucial to be considered to accurately and realistically determine the contribution towards drag force experienced. C_W known the theoretical wave drag parameter which depends on the wing geometry and Mach number can be acquired through graph shown in Appendix A. AR is the aspect ratio of the wing, ϕ is the wing sweep correction factor which depends on the wing geometry. Lastly, K_{pr} is the constant factor for a given sharp-nose profile of the wing, as for the single-wedge SSM configuration wing used in this study, where K_{pr} = 0.25 [6].

$$C_{Dw} = C_w A R t_{max}^{-2} [1 + \phi(K_{pr} - 1)] \quad (3)$$

2.1.3. Base drag coefficient

Base drag component accounts only for wings with base, such as single-wedge wing in this study. At supersonic speed, the base drag coefficient C_p is related to the average base thickness across the wing $\bar{t}_{base}$. The base drag coefficient can be obtained through graphs produced [5] as a function to Mach number.

$$C_{Db} = -(C_p)\bar{t}_{base} \quad (4)$$

For calculations when Ma < 1 at subsonic, the drag components consists of pressure drag and skin friction drag only. Hence the total drag component now only consist of parasite drag which is associated with pressure and skin friction component. The parasite drag can be determined by incrementing the flat plate skin friction factor k. S_{wet} is the wetted surface area of the wing exposed to fluid flow and C_f skin friction coefficient which can be found through graph by [11]

and Eqs. (2). Lastly the *k* factor is formulated in the equation below from a series of graph at [11] and can be calculated using formula below:

$$C_{D\ Parasite} = kC_f S_{wet} \tag{5}$$

$$k = 1 + \frac{2C(\bar{t}_{max})(cos\,\Lambda_{LE})^2}{\sqrt{1-Ma^2\,(cos\,\Lambda_{LE})}} + \frac{C^2\Lambda_{LE}(\bar{t}_{max})^2(1+5\,(cos\,\Lambda_{LE})^2)}{2(1-Ma^2\,(cos\,\Lambda_{LE})^2} \tag{6}$$

The coefficient *C* in the *k* factor equation can be determined by the conditions where if $M \cos \Lambda_{LE} > 1$ then $C = 0$ otherwise $C = 1.1$ [11]. Hence, by relating all the equations and graphs, data can be extracted through interpolation which is usually time consuming to carry out manually were computationally determined. Furthermore, in order to increase the accuracy of the analysis, small time intervals are required which requires the entire process to be looped for more than 3000 intervals. This causes the entire process to be extremely time-consuming also results significant cost to be analysed manually. The computer program developed in-house through MATLAB is designed to loop the entire calculation process until certain requirement is met where decision can made along the calculation process depending on results and parameters generated from previous loop. The process also significantly reduces the time for analysis. Various results from the calculation can be plotted easily for visualization and comparison.

3. Computer Programme: Validation and Verification

The simulated results of the C_{D0} were compared with experimental wind tunnel data for validation. The model was analysed by Ferris [13] for subsonic up to transonic speed (0.6<Ma<1.20) and by Babb and Fuller [14] in the supersonic region (1.5<Ma<4.63) of a meteorological missile used for high-altitude research activity [13, 14]. The C_{D0} was determined by experimenting missile with and without fins at zero angle of attack (AOA). By comparing the C_{D0} of the missile with and without fins, contribution of fins alone can be estimated. The design of the wing used in the experiment is closely replicated in the MATLAB program. The aerodynamic properties were computed at same Mach number and at sea-level. Given the limitation of the MATLAB computer program especially at the subsonic and supersonic transition Mach number, the resultant plot is notably different at the peak C_{D0} during transonic. The difference in the shape of the wedged wing which is unable to be simulated using the developed program affects the drag characteristic especially at the transonic region where the simulated results produces the lower peak C_{D0}. Overall, the C_{D0} throughout the Mach number behaves similarly with the experimental results with close accuracy even at high Mach number. The travelling Mach number of the missile throughout the flight time is usually in subsonic or supersonic speed. The resultant C_{D0} of the fins alone is plotted and shown in Fig. 2.

As for the accuracy of the numerical analysis processes such as interpolation were validated through the comparison with manual calculations. Manual calculations were carried out at various intervals in order to ensure the program is reliable throughout the predetermined operational range.

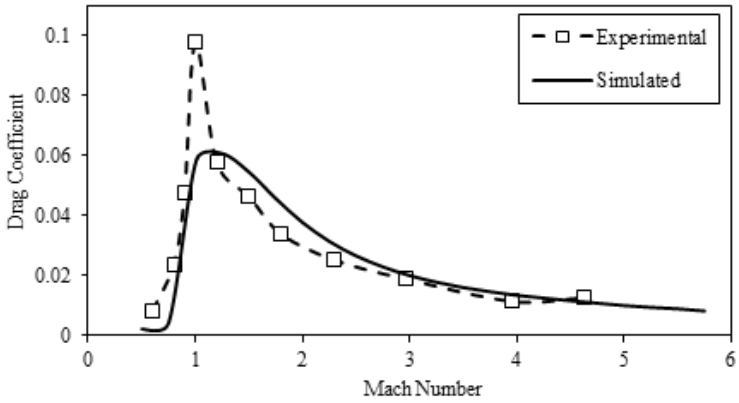

Fig. 2. Experimental and simulated drag coefficient as a function to Mach number.

4. Results and Discussion

The developed MATLAB program (details are explained in Appendix B) is used to numerically analyse the trajectory of the body. At the end of the routine, graphical plots were produced by using the output data generated by the program throughout the analysis. Table 1 shows the initial launching setup used for this analysis. The specification and setup used is based on the typical SSM missile in terms of weight, thrust and the angular control sequence during thrusted flight. Due to the versatility of the program developed, this means that analysis for different type of rocket or missile setup and specification can be carried out.

Table 1. Simulation parameter and initial condition setup.

Parameters	Setup
Initial position (*X,Y*)	(0,0) Sea-level
Launch angle	90 deg.
Wing geometry	SSM Configured
Fuel mass	300 kg
Total mass	400 kg
Angular control	Vane controlled

4.1. Zero-lift drag coefficient C_{D0}

Figure 3 shows the variation of drag coefficient of the wing with altitude. It is determined that drag coefficient of the wing increases with altitude. This is primarily due to the lower Reynold's number at higher altitude. This is caused by the increase in the kinematic viscosity (ν) of the atmospheric air as altitude increases. Kinematic viscosity is the ratio of dynamic viscosity (μ) to the density of the fluid. Although the dynamic viscosity of the atmospheric air increases with altitude, but the rate of density decreases significantly larger compared to dynamic viscosity. Hence, this causes the kinematic viscosity of the air to increase exponentially with altitude, which results the increase of overall C_{D0} with altitude, regardless of the difference in Mach number. Overall, the trend of C_{D0} is

still similar for each case of different altitude. However, the actual effect that is worth to be considered is the actual force acted upon the object.

Table 2 shows the percentage difference of C_D due to altitude change. It can be seen that C_D increases by 10.83% at 25 km above sea-level, 45.8% at 50 km whereas at 75 km, C_D increases by 139.24%, which is more than doubled.

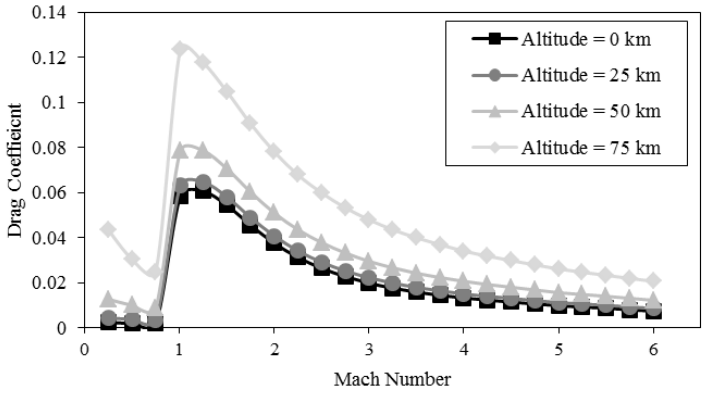

Fig. 3. Drag coefficient at different altitudes of an SSM wing.

Table 2. Difference of Drag Coefficient with altitude.

Altitude (km)	Average C_D	Difference (%)
0 (Sea-level)	0.0219	0
25	0.0243	+10.83
50	0.0319	+45.80
75	0.0524	+139.24

4.2. Comparison between different drag consideration

Figure 4 shows the resulted trajectory plot for the different assumption of drag where, Drag = *0*, Drag = *Constant* and Drag = *f (Altitude, Mach number)*. When Drag = 0, the trajectory plot shows the missile travel significantly further compared to the other two cases when drag is considered. This show the effects of drag alone significantly differ and restrict the projectile of the missile. The other trajectory which shows the body landed the nearest to the launching location is when drag is considered as a constant value which was set at a maximum for both C_{D0} and ρ of 0.0219 and 1.225 kg/m^3. This means that during flight, the body experiences constant air density set at sea level which is also the maximum in the earth's atmosphere and not as a function to Mach number where the effect of shockwave is not considered. The third analysis shows that the missile landed in-between the ideal trajectory and the trajectory when drag is constant. This trajectory is the main output of this study which is to analyse the effects of the changing flight condition caused by altitude on C_{D0} and ρ to the overall trajectory. It is clear that the body is able to travel much further compared to when C_{D0} and ρ is considered as constant but not as far as when drag is not taken into account.

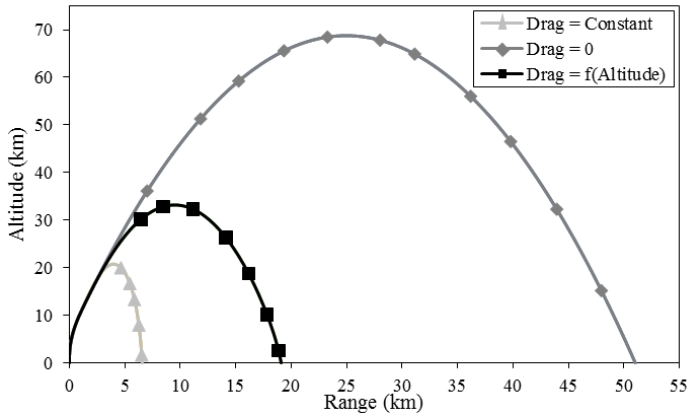

Fig. 4. Simulated trajectory for different consideration of drag.

The comparison of the missile velocity when different drag consideration is simulated agrees with the analysis carried out on the trajectory previously. Figure 5 shows the velocity profile of the two simulated flight where C_{D0} and atmospheric air parameters are considered as a function to altitude and when C_{D0} is simulated as a constant value throughout the missiles entire flight time. During accelerated flight, there is not much of a difference between the two cases, the effects of C_{D0} as a function to altitude is not significant compared to the rate of decrease of air density with altitude. At the end of the thrusted flight, the peak velocity when C_{D0} is considered as constant is the highest, this is the result of not considering the increase of C_{D0} due to altitude. Following that, the remaining of the simulated flight shows that the missile travels with higher velocity as compared to the other simulation. This shows that it is not accurate to consider C_{D0} as a constant value as it changes with altitude and causes visible effect throughout the missile's flight time, especially when thrust is absent. As the missile accelerates, the effect of wave drag caused by shock wave during transonic speed significantly increases the C_{D0} hence drag force. The drag force of the simulated flight time is shown in Fig. 6 in the following section.

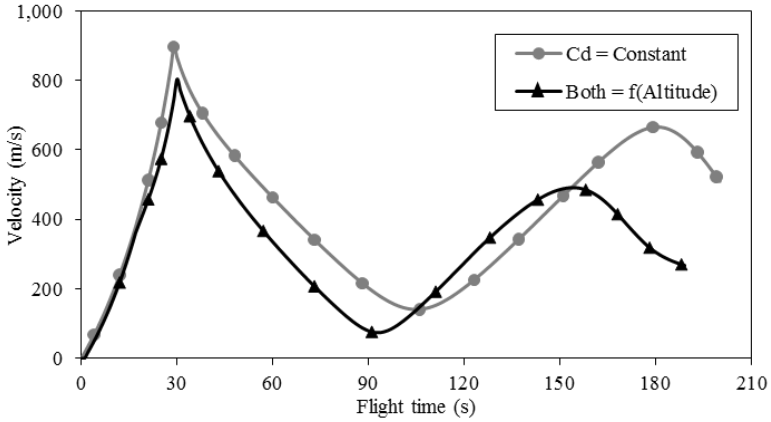

Fig. 5. Velocity profile of the simulated flights.

Figure 6 below shows the drag force experienced by the missile throughout the flight. The drag force experienced by the missile's flight depends on three factors, the travelling velocity, C_{D0} of the wing and the density of the air. As determined in Fig. 4, the simulation where C_{D0} is at minimum and constant travels with much higher velocity compared to the other cases. This relates to the drag force experienced by the missile. When C_{D0} is constant, the effect of shock wave is not considered into the analysis; hence drag force is significantly lower and does not cause a spike in drag force when the missile is travelling at transonic speed. This also results higher velocity as the missile is returning to earth due to the absence of shock wave.

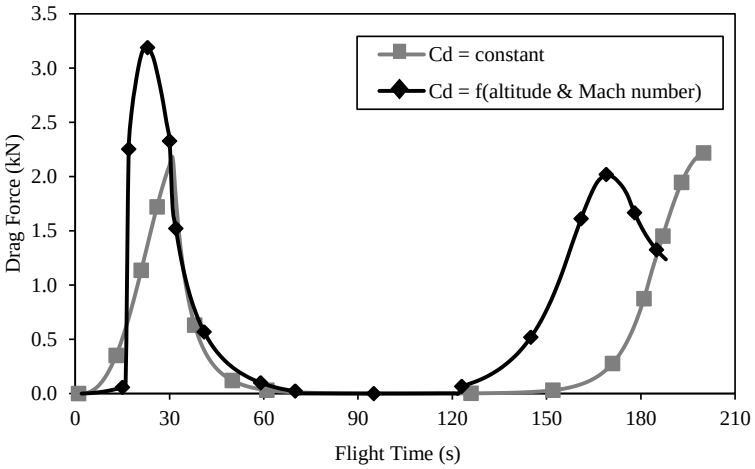

Fig. 6. Drag force of the simulated flights.

5. Conclusions

The effects of atmospheric altitude on the trajectory of the missile are studied and analysed in detailed. Results show that altitude does not only affect the atmospheric air parameters, but also C_{D0} of the body where it is determined depending on the geometrical shape, fluid conditions and Mach number. Through the graphical plotting of the trajectory, the consideration of the changing C_{D0} with altitude has drastic effect on the trajectory and also other flight performances. Hence it is important to fully consider the effects of altitude in order to determine accurate drag force experienced by a body.

At high altitude, C_{D0} of wing increases exponentially. As altitude increases, the atmospheric air parameter viscosity and density contributes the most in affecting the drag force throughout the flight. Hence, the combination effects of these factors are important to be considered when analysing for flight performance and trajectory.

The effect of the varying C_{D0} and atmospheric parameters with altitude shows the importance to consider drag as a function to altitude, velocity and wing geometry, which is visualized through trajectory analysis.

The conclusions that can be made to this study are summarized as:

- The developed program had been able to produce graphs which show realistic flight performance data as planned.
- Results show that C_D increases with altitude exponentially due to the effect of atmospheric air parameters which change with altitude.
- Trajectory plot which shows the consideration of the density as a function to altitude have greater effect on the overall trajectory compared to C_{D0}.
- The consideration of C_{D0} as a function to altitude also show obvious deviation of trajectory path compared to when C_{D0} is considered as constant.

References

1. Sandrey, M. (2009). *Aircraft performance: Analysis.* Chapter 3 Drag force and drag coefficient. VDM Verlag Dr. Müller.
2. US Department of Transportation, Faderal Aviation Administration (2008). *Pilot's Handbook of Aeronautical Knowledge (PHAK)*, 2-34.
3. Kroo, I. (2015). *Compressibility drag: Introduction*. Standford University.
4. Personnic, J.L.; Alam, F.; Gendre, L.; Chowdhury, H.; and Subic, A. (2011). Flight trajectory simulation of badminton shuttlecocks. *Procedia Engineering*, 13, 344-349.
5. Al-Obaidi, A.S.M. (2005). *The influence of configuration design on the aerodynamics and stability of SSM at supersonic speeds*. Ph.D. Thesis. Al-Rasheed College of Engineering and Science, University of Technology, Baghdad, Iraq.
6. Hoak, D.E. (1972). *USAF stability and control DATCOM*. Flight Control Division Air Force Flight Dynamics Laboratory.
7. Krasnov, N.F. (1985). *Aerodynamics*. Part 2: Methods of aerodynamic calculations. Moscow: Mir Publisher.
8. Lebedev, A.A.; and Chernobrovken, L.S. (1973). *Flight dynamics of pilotless of flight-vehicles (in Russian Language)*. Mashinostroenie, Moscow.
9. Jankovic, S. (1979). *Aerodynamics of projectiles (in Yugoslavian Language).* Masinski Fakultet, Univerziteta u Beogradu, Belgrade.
10. Bertin, J.J.; and Cummings, R.M. (2009). *Aerodynamics for engineer* (5th ed.). Upper Saddle River, New Jersey 07458: Pearson Education.
11. Petrovic, Z. (2002). *Elements of semi-empirical aerodynamics*. Private Communications.
12. Anderson, J.J.D. (2007). *Fundamentals of aerodynamics* (4th ed.). New York: McGraw-Hill.
13. Ferris, J. (1967). Static stability investigation of a single-stage sounding rocket at Mach number 0.60 to 1.20. *NASA-TN-D-4013*.
14. Babb, C.; and Fuller, D. (1961). Static stability investigation of a sounding-rocket vehicle at Mach number 1.50 to 4.63. *NASA-TR-R-100.*

Appendix A

Representation and Figures of Design Charts

In this study, various empirical and semi-empirical design charts are used to the prediction of aerodynamic characteristic of the wing. The origin design charts are taken from [6 - 9]. The curves acquired from the references are read and converted in to numerical data by Al-Obaidi [5]. These data which are in table form are used in the developed semi-empirical program. Data can be extracted by curve-spline interpolation available as a function in MATLAB which realistically estimates the desired value in between the given data points. The cubic-spline interpolation method is able to produce more realistic estimation by connecting two points with a smooth curve instead of a straight line when using linear interpolation.

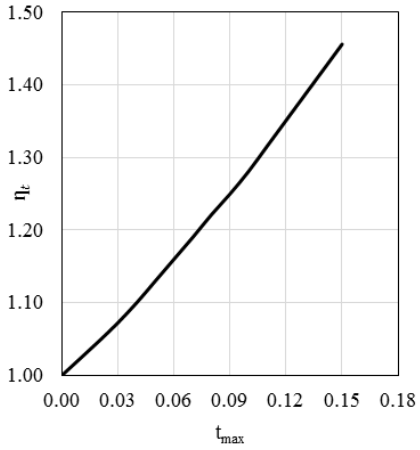

Fig. A-1. Effect of relative thickness on skin friction coefficient.

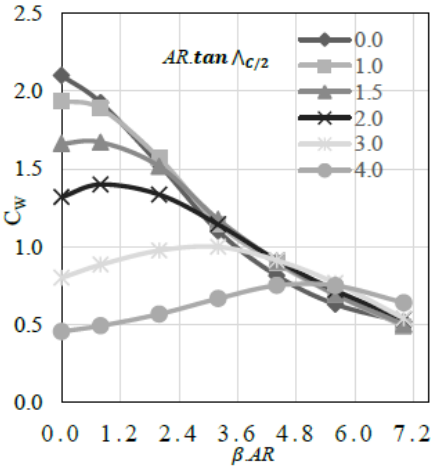

Fig. A-2(a).
Taper ratio, λ = 0.0

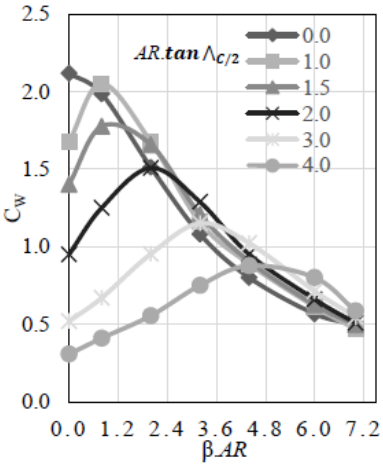

Fig. A-2(b).
Taper ratio, λ = 0.5

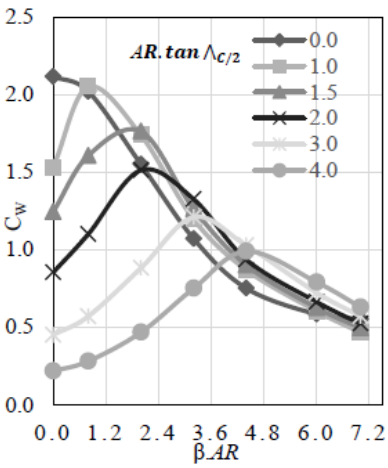

Fig. A-2(b).
Taper ratio, λ = 1.0

Theoretical wave drag parameter of wing for different taper ratios.

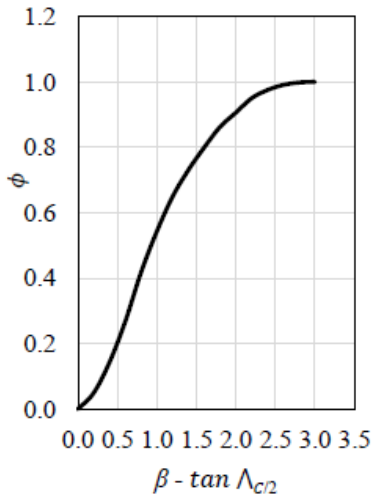

Fig. A-3.
Wing sweep correction factor.

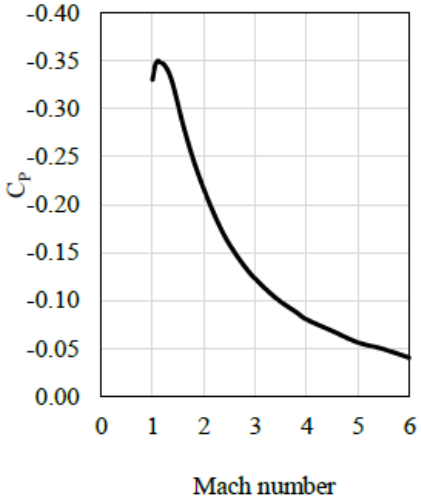

Fig. A-4.
Base pressure coefficient of wing.

Appendix B

Computer Programme

A computer code, for the prediction of projectile aerodynamic characteristics as a function of wing geometry, Mach number and altitude of flight, is developed in the present work. This programme is based on the analytical and semi-empirical methods presented in Section 2.

The computer programme can serve by calculating the forces acting on a projectile at a range of speeds, the programme is used in conjunction with both trajectory through solving the basic equations of motions at a predetermined interval of time.

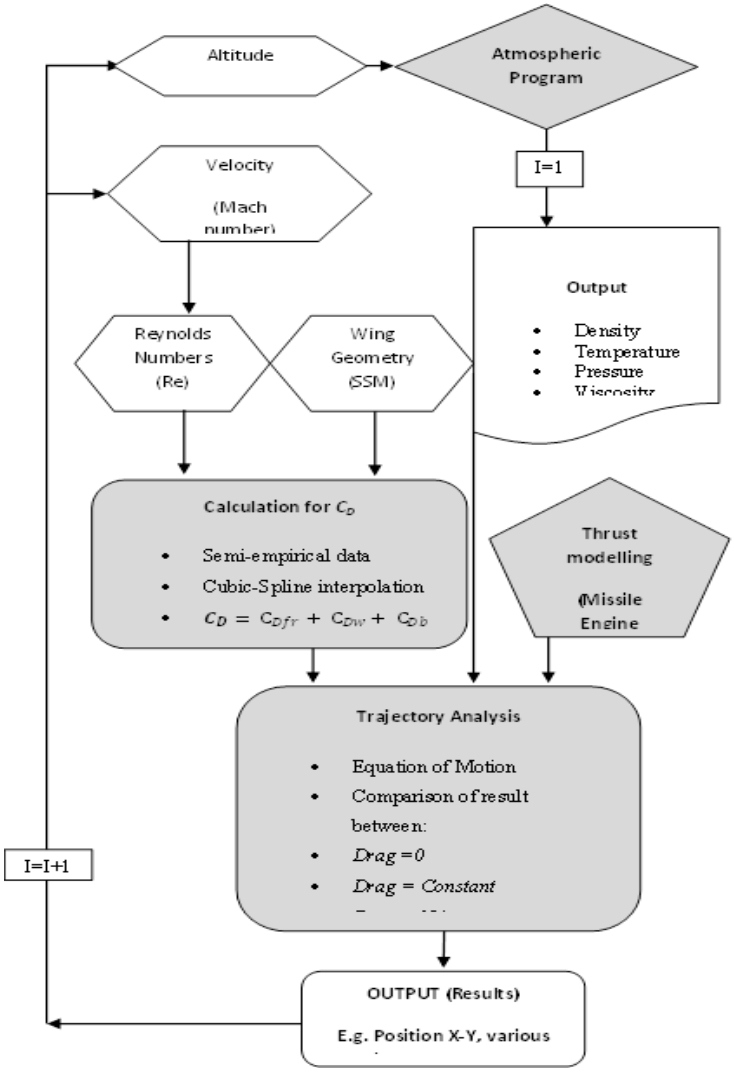

Fig. B. Main flow chart of the computer programme used in this study.